Response to Reviewer#2's Comments

General comments

This study produces CCAV-10m, an annual 10 m species-level coastal wetland vegetation dataset from 2016 to 2023, using a phenology-guided deep learning framework. The topic is well suited to Earth System Science Data, and the dataset is valuable for long-term monitoring of coastal wetland vegetation, invasive species expansion, and ecosystem management. The manuscript is generally well organized, and the reported classification performance is impressive. My comments mainly concern clarity, reproducibility, and several points of interpretation and presentation.

Response: We are sincerely grateful for the positive assessment of our work and the recognition of the value of the CCAV-10m dataset for long-term coastal wetland monitoring and ecosystem management. We also deeply appreciate the reviewer's professional and detailed comments concerning the clarity, reproducibility, and several points of interpretation and presentation. These insights have been invaluable in refining the manuscript and ensuring the robustness of our data product. In response to the reviewer's suggestions, we have conducted a thorough revision of the manuscript to enhance its technical transparency and geographic accuracy. After careful consideration, we have implemented the suggested changes to improve the overall quality of the manuscript. We trust that these revisions will meet your expectations. Detailed point-by-point responses to your comments are outlined below.

Major comments

Comment 1: The dataset is valuable and timely, but the methodological description could be more reproducible. The manuscript provides a reasonably clear description of the P_SVCN framework, including the dual-branch design, the SAR–optical fusion strategy, and the attention-based architecture. However, the actual training procedure remains insufficiently described. I therefore suggest that the authors add a concise but explicit description of the model training procedure. This could include, where applicable, the loss function, optimizer, learning rate, stopping criterion, and software framework used. These details are important because the novelty of the manuscript partly lies in the deep learning framework itself.

Response M1: We genuinely appreciate your constructive suggestion regarding the technical

transparency of our work. We entirely agree that detailed training configurations are essential for experimental reproducibility; therefore, we have added a new Section 3.4.4, titled "Model Training and Implementation Details," to the revised manuscript to provide a comprehensive description of the network configuration. This section now explicitly specifies the software framework, loss function, optimizer, initial learning rate, and the multi-step learning rate decay strategy employed in our study. Please see our revision in Lines 205 - 215 on page 11.

Lines 205-215**: **3.4.4 Model Training and Implementation Details

The proposed P_SVCN framework was implemented using the PyTorch deep learning library and trained on an NVIDIA GeForce RTX 4090 GPU. To optimize the network parameters for the classification of six coastal wetland vegetation types, we employed the Adam optimizer (Kingma and Ba, 2015) with a weight decay of 1×10^{-5} to provide regularization and enhance generalization. The initial learning rate was set to 1×10^{-4}, and the epsilon parameter (ϵ) for numerical stability was maintained at 1×10^{-8}.

To ensure stable convergence and prevent the model from becoming trapped in local optima during the fine-grained classification of multi-source Sentinel-1/2 data, a MultiStepLR scheduler was utilized. The learning rate was decayed by a factor of 0.1 (γ=0.1) at specified milestones, specifically at epochs 30, 60, and 90. The Cross-Entropy loss function was adopted as the objective function to minimize categorical errors across the six classes. The entire training process spanned 100 epochs with a mini-batch size of 32.

References

Kingma, D. P. and Ba, J.: Adam: A method for stochastic optimization, in: International Conference on Learning Representations (ICLR), San Diego, CA, USA, 2015.

Comment 2: The manuscript would benefit from clearer interpretation of dataset characteristics and limitations. The manuscript reports good classification performance for the CCAV-10m dataset, and the proposed P_SVCN model shows higher accuracy than the previous SVCN model. I suggest that the authors add more discussion of the mechanisms or characteristics of the P_SVCN model that may explain its better performance. At the same time, since coastal wetland vegetation is strongly affected by tides, salinity gradients, and phenological variation, the discussion should more explicitly address how these factors may still influence uncertainty or local misclassification. In Figure 7, the results suggest large interannual variations in the area of some species, for example, *P. australis* and *Suaeda spp.* in Liaoning from 2022 to 2023, and *Suaeda spp.* in Shandong before and after 2020. Do these large interannual variations reflect real-world changes, or might they be influenced by uncertainties or local misclassifications? The manuscript already acknowledges these issues to some extent, but the discussion could be strengthened by linking them more directly to dataset quality and potential limitations in application.

Response M2: We are grateful for your constructive suggestions regarding the interpretation of model mechanisms and the analysis of interannual variations. Regarding the superior performance of the P_SVCN model, we have added a discussion in the revised manuscript explaining that its primary advantage over the previous SVCN model lies in its phenology-guided feature extraction mechanism. By integrating dual-temporal spectral signatures that capture the distinct "green" and "senescence" stages of coastal vegetation, the P_SVCN model effectively enhances the separability of species with similar peak-growing season spectra, such as S. alterniflora and *P. australis*. This approach allows the model to leverage diagnostic phenological shifts to achieve more robust classification. Please see our revision in Lines 292-303 on page 16.

> ***Lines 292-303****: This marked performance leap is fundamentally attributed to the synergistic integration of multi-temporal optical phenology and Synthetic Aperture Radar (SAR) structural attributes within the P_SVCN architecture. In contrast to the SVCN model, which relies exclusively on Sentinel-1 SAR backscattering coefficients (σ°), P_SVCN introduces multi-temporal optical observations to construct a high-dimensional Phenological-Spectral Vector (PSV).*
>
> *Within complex coastal wetland ecotones, discriminating between vegetation species with analogous physical architectures is inherently constrained when relying solely on SAR observations. Furthermore, radar backscatter is highly susceptible to fluctuations in the surface dielectric constant induced by periodic tidal inundation. P_SVCN effectively circumvents the information bottleneck of single-source radar data by utilizing the PSV to characterize species-specific growth trajectories—most notably the distinctive "red beach" spectral signature of Suaeda spp. during the senescence stage (Phase 2). Simultaneously, the*

framework preserves the deterministic advantages of SAR in characterizing canopy volume and biomass. By leveraging a multi-source attention mechanism, P_SVCN facilitates dynamic complementarity between the optical "biological fingerprint" and the radar derived "physical structure," thereby substantially mitigating classification uncertainty.

We sincerely appreciate the reviewer's insightful comments. Environmental factors—such as tidal inundation, salinity gradients, and phenological variations—indeed exert a significant influence on coastal wetland classification, and we agree that these factors should be more explicitly linked to classification uncertainties. Regarding the substantial interannual variations observed in Liaoning (2022–2023), our post-hoc diagnostic analysis using regional meteorological data confirms that these abrupt shifts are "environmental artifacts" driven by extreme hydrometeorological events rather than real-world ecological successions. Specifically, back-analysis reveals that the Liaoning coastal zone was struck by the consecutive impacts of Typhoons Doksuri and Khanun between August and September 2023, resulting in rare extreme precipitation and prolonged inundation.

(1) Physical Submergence and Spectral Masking: *Suaeda spp.* is a low-stature species that was easily submerged by the resulting flooding during its critical "red beach" phenological window (Phase 2). The strong near-infrared (NIR) absorption of the overlying water, as indicated by the significantly higher NDWI in 2023 (Fig. 8b), severely dampened and distorted its diagnostic spectral signature. This led to a substantial Signal-to-Noise Ratio (SNR) degradation, causing the model to misclassify these submerged pixels as non-vegetated surfaces or water-saturated soil.

(2) Atmospheric Constraints and Observation Gaps: The persistent storm systems in 2023 also led to a surge in regional cloud cover. Statistical analysis (Fig. 8a) shows that the mean cloud cover during Phase 2 reached 41.2% in 2023, markedly exceeding 2022 levels. Although our 10% cloud-cover threshold was maintained for scene selection, the clear-sky observation frequency during the peak phenological window was extremely limited in 2023. This scarcity of high-quality pixels forced the model to rely on sub-optimal or temporally offset observations, hindering its ability to capture fine-grained phenological trajectories and resulting in localized omission errors.

Please see our revision in Lines 378–410 on pages 21-22.

***Lines 378-410**: 5.4 Limitations of the CCAV-10m dataset*

While the CCAV-10m dataset demonstrates high overall thematic fidelity, localized inter-annual fluctuations in species distribution (as illustrated in Fig. 7) necessitate a rigorous interpretation within the context of complex environmental background fields. The spatial distribution and spectral identification of coastal wetland vegetation are profoundly influenced by tidal regimes, salinity gradients, and phenological dynamics (Murray et al., 2022). Tidal inundation typically attenuates reflectance in the near-infrared (NIR) spectrum, frequently leading to the omission of low-stature vegetation due to water-induced signal absorption (Kearney et al., 2009). Simultaneously, spatial variations in salinity gradients can alter the biophysical parameters of P. australis, inducing localized spectral deviations that exacerbate the risk of confusion with invasive species such as S. alterniflora (Zhou et al., 2021; Cingano et al., 2025).

A prominent case study is the observed abrupt fluctuations of P. australis and Suaeda spp. along the Liaoning coast between 2022 and 2023. Meteorological back-analysis reveals that these shifts are not indicative of actual ecological succession but are instead "environmental

artifacts" induced by extreme hydrometeorological anomalies. From August to September 2023, the Liaoning coastal zone was struck by the consecutive impacts of Typhoons Doksuri and Khanun, which triggered rare and catastrophic precipitation events (Service, 2023).

This extreme climate directly compromised the classification logic through two primary mechanisms. First, the physical submergence and subsequent spectral masking. Since Suaeda spp. is a low-stature species with a typical height of less than 30cm, it is highly susceptible to complete submergence by typhoon-induced storm surges and inland flooding. During the critical "red beach" phenological window in 2023, record-breaking rainfall caused widespread surface water pooling. The regional mean NDWI increased from -0.041 in 2022 to -0.029 in 2023, confirming a significant intensification of the moisture signal (Fig. 8b). This hydrological stress led to strong NIR absorption by the overlying water, which severely dampened the diagnostic. spectral signatures of the vegetation and reduced the Signal-to-Noise Ratio (SNR). Consequently, the extracted phenological profiles underwent major distortions that resulted in localized omission errors.

Second, the interplay between atmospheric constraints and observation gaps. The persistent storm systems associated with these typhoons triggered a surge in regional cloudiness. Mean cloud cover during the two critical phases reached 50.76% and 41.25%, respectively (Fig. 8a). Although we maintained a 10% cloud-cover threshold for scene selection, the sheer frequency of cloudy days in 2023 drastically curtailed the availability of high-quality "clear-sky" pixels during the peak phenological stages. This scarcity forced a reliance on temporally offset or sub-optimal observations, which hindered the capacity of the model to accurately reconstruct fine-scale phenological trajectories (Cingano et al., 2025). As a result, the distinctive spectral contrast of coastal vegetation was partially compromised by increased atmospheric noise and reduced observation frequency.

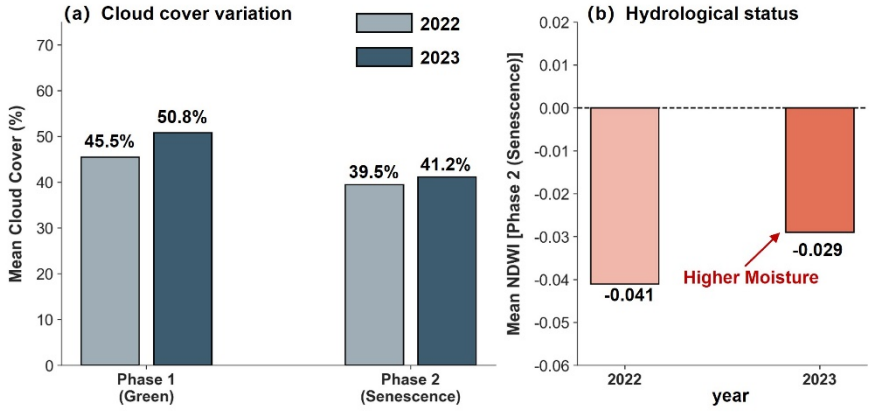

Figure 8. ***Comparative analysis of environmental constraints in the Liaoning coastal zone (2022–2023).*** *(a) Atmospheric Constraints: Mean cloud cover (%) during the green (Phase 1) and senescence (Phase 2) stages. (b) Hydrologic Signal: Mean Normalized Difference Water Index (NDWI) during Phase 2 (senescence).*

The CCAV-10m dataset possesses inherent limitations during climatically anomalous years, where the "observable area" may deviate from the "actual distribution" due to environmental noise. Future iterations of the CCAV-10m framework will prioritize the

integration of SAR-derived inundation masks and multi-source high-frequency data fusion to effectively decouple ecological evolutionary signals from short-term environmental noise within complex coastal ecotones.

References

Murray, N. J., Worthington, T. A., Bunting, P., Duce, S., Hagger, V., Lovelock, C. E., Lucas, R., Saunders, M. I., Sheaves, M., Spalding, M., et al.: High-resolution mapping of losses and gains of Earth's tidal wetlands, Science, 376, 744–749, 2022.

Kearney, M. S., Stutzer, D., Turpie, K., et al.: The effects of tidal inundation on the reflectance characteristics of coastal marsh vegetation, Journal of Coastal Research, 25, 1177–1186, 2009.

Zhou, D., Ni, Y., Yu, X., Lin, K., Du, N., Liu, L., Guo, X., and Guo, W.: Trait-based adaptability of Phragmites australis to the effects of soil water and salinity in the Yellow River Delta, Ecology and Evolution, 11, 11 352–11 361, 2021.

Cingano, P., Moro, D., Pellegrini, E., Asquini, E., Contin, M., Trotta, G., Vuerich, M., Trevisan, F., Scagnetto, I., Casarsa, L., et al.: Integrating remote sensing and functional traits to elucidate estuarine common reed beds decline driven by soil salinity and anoxia, Ecological Indicators, 180, 114 294, 2025.

Service, L. P. M.: Main Meteorological Disasters and Early Warning Signals in Liaoning Province, August 2023, Meteorological bulletin, Liaoning Provincial Meteorological Service, Shenyang, http://ln.cma.gov.cn/xwzx/qxxw/202309/t20230905_5757479.html, released on 2023-09-05, 2023.595

Specific comments and suggestions

Point 1: Since the study area only covers eight coastal provinces and does not include Guangdong, Guangxi, or Hainan. I suggest revising the title to make the spatial coverage more precise, for example, by using "eastern coastal China" rather than "China".

Response 1: We sincerely thank you for this constructive suggestion regarding the spatial precision of our study. We agree that the term "China" in the original title was overly broad, as our current data production focuses on the eight coastal provinces and municipalities from Liaoning to Fujian, excluding Guangdong, Guangxi, and Hainan. To ensure the title accurately reflects the geographic scope of the CCAV-10m dataset, we have followed the reviewer's advice and revised the title to: "**CCAV-10m: An Annual Spatiotemporal Dataset for Eastern Coastal China's Wetland Vegetation by Integrating Sentinel-1/2 Observations via Deep Learning**". This change more precisely defines the study area and avoids potential overgeneralization. We have ensured that this revised title and the clarified geographic scope are updated consistently throughout the manuscript, including the Abstract, Section 5.1(The CCAV-10m dataset: Filling a critical gap in coastal wetland vegetation mapping), and Section 6 (Conclusions).

Please see our revisions in: Title and Abstract: Page 1, Lines 1-13. Section 5.1: Page 17, Lines 306–

310. Section 6: Page 23, Lines 412–416.

> ***Lines 1-13****: Abstract. Coastal wetland vegetation plays a vital role in shoreline protection and ecosystem management, highlighting the need for accurate and high-resolution mapping of these unique and vulnerable habitats. Here, we present CCAV-10m, the first publicly available annual species-level wetland dataset for eastern coastal China at 10 m resolution (2016–2023). This dataset was generated using a novel phenology-guided coastal wetland vegetation classification network (P_SVCN), which integrates Sentinel-1/2 satellite imagery with extensive in situ observations. Validation based on 4,668 in situ samples confirms that P_SVCN delivers strong classification performance, achieving an overall accuracy of 0.916 and a Kappa coefficient of 0.898. Spatiotemporal analysis of CCAV-10m reveals that Suaeda spp. is the dominant vegetation type, followed by Spartina alterniflora, whose coverage nearly equals the combined extent of Phragmites australis, mangroves, Scirpus mariqueter, and Tamarix chinensis. Notably, this work fills critical gaps in both spatial detail and temporal consistency across existing coastal wetland datasets, demonstrating the effectiveness of deep-learning-based fusion of optical and SAR data for high-resolution vegetation mapping. Regular updates to CCAV-10m will support long-term coastal wetland research, enhance invasive species monitoring, and inform wetland restoration and precision management efforts. The CCAV-10m dataset is openly accessible at https://doi.org/10.57760/sciencedb.31077 (Li et al., 2025).*
>
> ***Lines 306-310****: We introduce CCAV-10m, an annual 10m coastal wetland vegetation dataset generated using the P_SVCN model, which captures the spatial and temporal dynamics of eastern coastal China's wetland vegetation from 2016 to 2023. As the first publicly available species-level coastal wetland dataset for this region, CCAV-10m provides fine-resolution mapping of six representative vegetation types—S. alterniflora, P. australis, Suaeda spp., S. mariqueter, mangroves, and T. chinensis. Model evaluation demonstrates robust performance, with an overall accuracy of 0.916 and a Kappa coefficient of 0.898.*
>
> ***Lines 412-416****:This study developed a phenology-guided coastal wetland vegetation classification network integrating Sentinel-1/2 (P_SVCN) and generated the CCAV-10m dataset, which maps the wetland vegetation types in eastern coastal China from 2016 to 2023. By integrating multi-source Sentinel-1 SAR and Sentinel-2 MSI data, the P_SVCN fully exploits structural and phenological features, enabling accurate discrimination of spectrally similar and spatially fragmented vegetation types. The results are summarized as follows:*

Point 2: The manuscript states that 320 Sentinel-2 scenes were selected, which is much smaller than the number of Sentinel-1 scenes. Please clarify the criteria used for scene selection, such as acquisition timing and cloud coverage thresholds.

Response 2: We greatly appreciate your suggestion to clarify our data selection criteria. The discrepancy in the number of scenes between Sentinel-1 and Sentinel-2 is primarily due to the stringent cloud-shading filtering applied to optical data to ensure spectral purity.

For Sentinel-2, we implemented a maximum cloud coverage threshold of 10% at the scene level. Regarding acquisition timing, we specifically targeted two critical phenological windows for eastern China's coastal wetlands: the "green-up" stage and the "senescence" stage. Only images captured

within these windows that met the cloud-cover criteria were utilized to construct the dual-temporal composites. In contrast, since Sentinel-1 SAR observations possess all-weather capability and are independent of solar illumination or cloud conditions, we were able to utilize all available GRD (Ground Range Detected) products within the same periods. These were processed via annual mean compositing to maximize the signal-to-noise ratio. We have added these specific criteria to Section 3.2 (Sentinel-2) to enhance the technical transparency and reproducibility of our study.

Please see our revision in Lines 93–103 on page 5.

Lines 93-103**: **3.2 Sentinel-2

Sentinel-2 imagery was selected according to the key phenological stages of coastal vegetation, namely green and senescence (Zhao et al., 2023). To ensure high spectral fidelity, a stringent cloud-cover threshold of less than 10% was applied during the scene selection process. Across the study period, 320 high-quality scenes of dual-temporal optical imagery were processed in SNAP and ENVI, including resampling and band fusion (Wang et al., 2024). Distinct from the year-round continuous observation strategy employed for Sentinel-1 SAR data, this targeted sampling of dual-phase optical imagery aims to capture the maximum inter-species spectral contrast while minimizing atmospheric interference.

For each phenophase, four spectral bands with the highest vegetation contrast—B02 (blue), B03 (green), B04 (red), and B08 (near-infrared)—were extracted, yielding eight optical channels (Bao et al., 2025). Normalized Difference Vegetation Index100 (NDVI) maps were derived from the red and near-infrared bands of both phenophases to capture differences in vegetation status. All SAR and optical images were co-registered and resampled to a consistent 10 m resolution to ensure data alignment and comparability.

Point 3: Line 111-113: The description of the manually interpreted and field-based samples is useful, but I suggest adding a clearer visual summary of their spatial distribution in the supplementary material. A map would improve transparency.

Response 3: We sincerely thank you for this constructive suggestion. We agree that a visual representation of the spatial distribution of samples is essential for validating the reliability and representativeness of the dataset. Accordingly, we have added a new map to the Appendix (Figure C1), illustrating the geographic distribution of all 15,558 manually interpreted and field-based samples across the eight coastal provinces and municipalities of eastern China. Please see our revision in Lines 470–473 on pages 25-26.

Lines 470-473**: **Appendix C: Spatial Distribution of Samples

To ensure the transparency and reliability of the CCAV-10m dataset, we provide a visual summary of the spatial distribution of the samples used for model training and validation. A total of 15,558 samples were collected through a combination of field surveys and high-resolution manual interpretation of Google Earth.

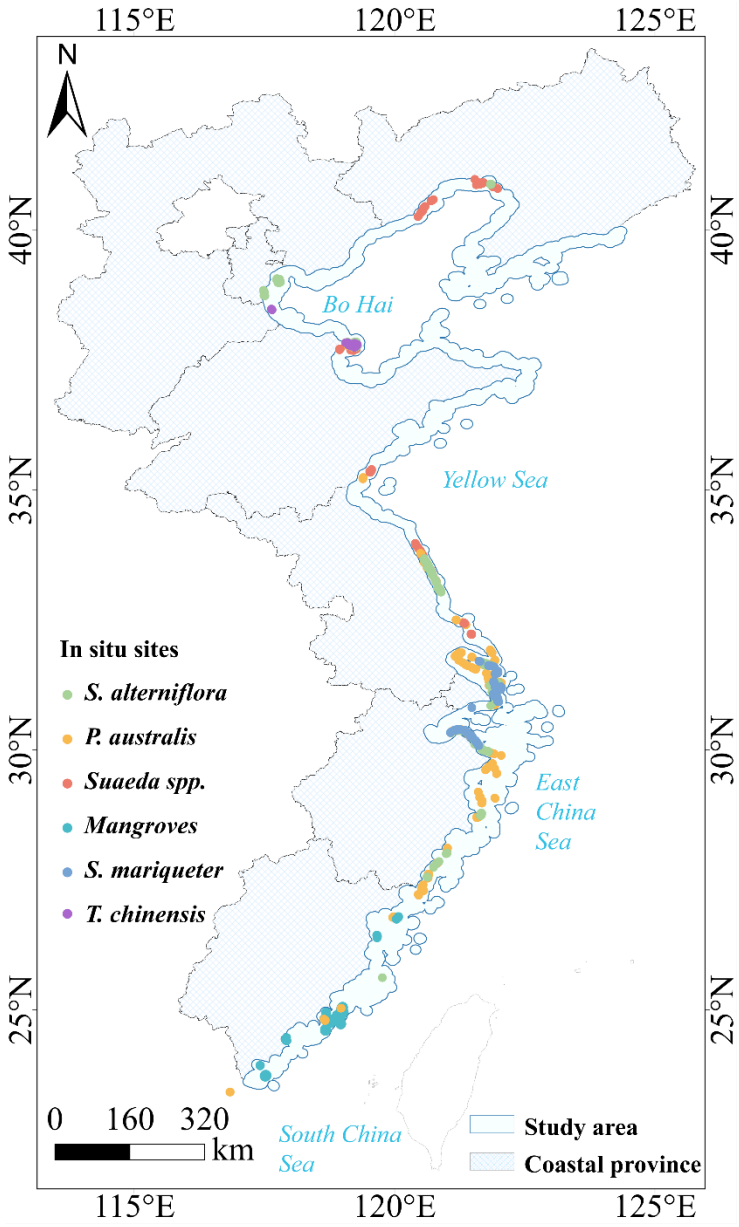

Figure C1. Spatial distribution of samples

Point 4: Figure 2: Does each line represent the NDVI of one representative plot, or the average NDVI of all wetlands within that region? Also, why is the NDVI time series of *S. alterniflora* in Figure 2(c) discontinuous?

Response 4: We value the opportunity to clarify the presentation of the phenological data in Figure 2. First, each spectral curve in Figure 2 represents the average NDVI value derived from all validated samples of a specific vegetation type within the corresponding region, rather than the values of a single representative plot. Second, the discontinuity in the NDVI time series for *S. alterniflora* in Figure 2(c) stems from our stringent data quality control procedures. To ensure the reliability of the

phenological profiles, we excluded Sentinel-2 observations affected by heavy cloud cover (scene-level cloud > 10%) and tidal inundation. The data gaps in the time series correspond to periods during which no high-quality, cloud-free imagery was available.

We have updated the caption of Figure 2 to explicitly define these curves and explain the causes of the data gaps. Please see our revisions on Page 8, Figure 2.

Figure 2:

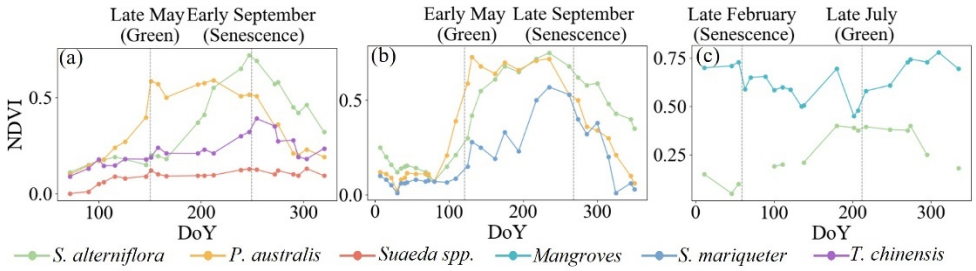

Figure 2. Seasonal NDVI of dominant coastal wetland vegetation along the coast of eastern China. (a) Temperate, (b) North Subtropical, and (c) Subtropical zones. Each profile represents the mean NDVI calculated from all validated samples within the respective region. Distinct annual NDVI variations were observed among the main vegetation types (S. alterniflora, P. australis, Suaeda spp., S. mariqueter, T. chinensis, and mangroves), which guided the dual-phase selection summarized in Tab 1. Note that temporal gaps in the S. alterniflora profile in (c) are due to the exclusion of low-quality pixels caused by frequent precipitation and tidal inundation in low-latitude regions, ensuring the purity of phenological signatures.

Point 5: It would be helpful to clarify whether the reported validation design is entirely sample-based or whether there was also any spatial separation to reduce possible spatial autocorrelation between training and validation samples.

Response 5*: We sincerely thank you for the profound insights regarding the robustness of the validation design and the potential impact of spatial autocorrelation. We fully agree that ensuring the independence between training and validation samples is crucial for assessing the generalization capability of large-scale coastal wetland classification models.*

In response to this suggestion, we have clarified our validation strategy in the revised manuscript. The sample partitioning followed the principle of stratified random sampling based on both vegetation classes and geographic regions. First, we stratified the samples by vegetation type at a national scale to ensure the validation set is representative across all vegetation categories. Second, considering the latitudinal variations in coastal vegetation across China, we ensured that validation samples were distributed across different latitudinal zones along the coastline of Eastern China.

Please refer to the revised manuscript at Page 15, Lines 272-274 for these modifications.

***Lines 272-274**: A total of 15,558 in-situ data points were collected across eastern China's coastal wetlands and partitioned into training (70%) and validation (30%, n = 4,668) sets following a stratified random sampling principle based on both vegetation types and geographic regions.*

Point 6: Figure 4: The left panel appears to show mangroves in Hangzhou Harbor. Do mangroves actually exist there?

Response 6: We sincerely thank you for this rigorous geographical check. We have conducted a comprehensive re-examination of our field survey records and established botanical literature regarding the distribution of mangroves in China. **(1) Geographical Verification**: We confirm that the recognized northernmost limit for both natural and afforested mangroves in China is Yueqing City (approx. 28°N) in southern Zhejiang Province. Our investigation confirms that no mangroves exist in Hangzhou Bay, as the winter temperatures there frequently fall below the biological tolerance threshold of even the most cold-resistant species (e.g., Kandelia obovata). **(2) Root Cause Analysis:** The small patches erroneously identified as mangroves in Figure 4 are indeed localized misclassifications. This "out-of-range" error stems from a rare convergence of spectral and structural signatures: in certain salt-stressed transition zones, dense *S. alterniflora* can exhibit SAR backscatter and dual-phase phenological trajectories (green-up to senescence) that overlap with mangrove signatures within the 10m feature space. **(3) Strategy for Improvement**: We have added a concise discussion regarding these errors in Section 5.3 of the revised manuscript. We recognize that while the P-SVCN model is statistically robust, it currently lacks biogeographic constraints. In future iterations of the CCAV-10m dataset, we plan to implement a Knowledge-Guided Post-processing (KGPP) module. By integrating a "biogeographic sieve" based on latitudinal limits, minimum temperature isotherms, precipitation patterns, and sea surface salinity (SSS), we can effectively filter out such biologically inconsistent results and further bolster the dataset's spatial reliability.

Please see our revision in Lines 368-377 on page 20.

***Lines 368-377**: Nevertheless, residual uncertainties persist. First, T. chinensis and Suaeda spp. are often interspersed in the upper wetland, with similar temporal and phenological characteristics (Gao et al., 2015; Jiao et al., 2021; Wu et al., 2020), making complete discrimination challenging even under multi-source fusion. Second, S. mariqueter has a narrow and highly patchy distribution (Gu et al., 2021), which may result in omission errors under 10 m resolution. Third, despite the overall robustness of the model, localized "out-of-range" misclassifications were observed (e.g., mangrove patches erroneously identified in Hangzhou Bay, exceeding their northern distribution limit).*

Future studies could integrate higher-resolution SAR data (e.g., TerraSAR-X, GF-3) and incorporate geographic prior knowledge—such as latitudinal distribution limits and climatic thresholds—as spatial constraints in the post-processing phase. Such a knowledge-guided approach will effectively filter out biologically inconsistent errors and further enhance the spatial reliability of coastal wetland mapping.

References

Gao, M., Wang, X., Hui, C., Yi, H., Zhang, C., Wu, X., Bi, X., Wang, Y., Xiao, L., and Wang, D.: Assembly of plant communities in coastal wetlands—the role of saltcedar Tamarix chinensis during early succession, Journal of Plant Ecology, 8, 539–548, https://doi.org/10.1093/jpe/rtu037, 2015.

Jiao, L., Zhang, Y., Sun, T., Yang, W., Shao, D., Zhang, P., and Liu, Q.: Spatial analysis as a tool for plant population conservation: A case study of Tamarix chinensis in the Yellow River Delta, China, Sustainability, 13, 8291, https://doi.org/10.3390/su13158291, 2021.

Wu, Y., Dai, L., Wang, Y., Xie, L., Zhao, S., Liu, Y., Zhang, M., and Zhang, Z.: Coexistence mechanisms of Tamarix chinensis and Suaeda salsa in the Yellow River Delta, China, Environmental Science and Pollution Research, 27, 26 172–26 181, https://doi.org/10.1007/s11356-020-08883-1, 2020.

Gu, J., Jin, R., Chen, G., Ye, Z., Li, Q., Wang, H., Li, D., Christakos, G., Agusti, S., Duarte, C. M., et al.: Areal extent, species composition, and spatial distribution of coastal saltmarshes in China, IEEE Journal of Selected Topics in Applied Earth Observations and Remote Sensing, 14, 7085–7094, https://doi.org/10.1109/JSTARS.2021.3093673, 2021.